Science in China Series D: Earth Sciences

A semi-implicit semi-Lagrangian global nonhydrostatic model and the polar discretization scheme

YANG XueSheng[1†], CHEN JiaBin[2], HU JiangLin[1], CHEN DeHui[1], SHEN XueShun[1], ZHANG HongLiang[1]

[1] State Key Laboratory of Severe Weather, Chinese Academy of Meteorological Sciences, Beijing 100081, China;
[2] State Key Laboratory of Numerical Modeling for Atmospheric Sciences and Geophysical Fluid Dynamics, Institute of Atmospheric Physics, Beijing 100029, China

The Global/Regional Assimilation and PrEdiction System (GRAPES) is a newly developed global nonhydrostatic numerical prediction model, which will become the next generation medium-range operational model at China Meteorological Administration (CMA). The dynamic framework of GRAPES is featuring with fully compressible equations, nonhydrostatic or hydrostatic optionally, two-level time semi-Lagrangian and semi-implicit time integration, Charney-Phillips vertical staggering, and complex three-dimensional pre-conditioned Helmholtz solver, etc. Concerning the singularity of horizontal momentum equations at the poles, the polar discretization schemes are described, which include adoption of Arakawa C horizontal grid with v at poles, incorporation of polar filtering to maintain the computational stability, the correction to Helmholtz equation near the poles, as well as the treatment of semi-Lagrangian interpolation to improve the departure point accuracy, etc. The balanced flow tests validate the rationality of the treatment of semi-Lagrangian departure point calculation and the polar discretization during long time integration. Held and Suarez tests show that the conservation properties of GRAPES model are quite good.

nonhydrostatic, global model, semi-implicit, semi-Lagrangian, polar discretization, conservation

In last two decades, the world major operational centers, research institutes and universities mostly adopt global spectral models, including European Center for Medium-range Weather forecast (ECMWF)[1], National Centers for Environmental Prediction (NCEP)[2], Meteo France[3], Japan Meteorological Agency (JMA), Institute of Atmospheric Physics[4] and National Meteorological Centre of CMA[5,6], etc.

In recent years, with the rapid development of high-performance computers, the resolution of global models run at most operational centers has been increased significantly. According to annual report provided by the World Meteorological Organization (WMO), the horizontal resolution of global operational models will be enhanced to 25 KM in the next 3 years. But with the increased resolution, the spectral models gradually show its limitations[7], for example, it requires that variables should be defined on continuous coordinates, while the condensation heating process and topography may be isolated or non-continuous, thus creating fictitious Gibbs effects over flat plains and oceans. In fact, the spectral approach which adopted to avoid this aliasing is a pseudo-spectral transformation. Currently, the truncated wave number is already quite high, and if the resolution is increased further, it will be less effective comparing the additional calculation workload with the acquired accuracy.

Generally, the available spectral models tend to adopt hydrostatic assumption. If the model resolution is not

Received April 20, 2007; accepted June 27, 2007
doi: 10.1007/s11430-007-0124-7
†Corresponding author (email: yangxs@cma.gov.cn)
Supported by the Ministry of Science and Technology of China (Grant Nos. 2006BAC02B01 and 2006BAC03B03), the National High Technology Research and Development Program of China (863 Program) (Grant No. 2006AA01A123)

too high, the hydrostatic approximation can effectively filter out high frequency vertically propagating acoustic waves and inhibit their development and propagation. However, hydrostatic approximation is only valid when the ratio of vertical to horizontal scale is relatively small. When the resolution is less than 10 KM, the hydrostatic assumption will become unsuitable. With advent of high-performance computers, the computation power is no longer a major factor that constrains model development and resolution increase. Thus, taking the future operational demands into account, global models developed in late 20th century mostly introduce grid-point nonhydrostatic approximation scheme. For example, Meteorological Office of United Kingdom (UKMO)[8], Canadian Meteorological Center (CMC)[9] developed a new generation of nonhydrostatic model and put into operation, producing very encouraging outcomes. In recent years, Japan Meteorological Research Institute (MRI), National Center for Atmospheric Research (NCAR) and Meteo France have also launched the project to develop global nonhydrostatic models, in which semi-implicit and semi-Lagrangian scheme is widely used in order to take longer time step.

Based on the above, Chinese Academy of Meteorological Sciences (CAMS) of CMA began to develop a grid point medium-range global numerical prediction model named GRAPES from 2002. For such a global grid point model, the treatment of polar region is always a tough issue. On the one hand, the pole is a singular point, on the other hand the meridians converge and the physical distance over which becomes smaller and smaller as the pole is approached. Therefore, polar discretization must be addressed properly, especially for a grid point model that adopts semi-implicit and semi-Lagrangian scheme. Wang et al.[10] developed a grid-point global hydrostatic model named GAMIL, which uses an equal-area mesh that effectively alleviates the high frequency oscillations in the polar regions. While GEM model[9] developed in CMC employs variable resolution approach.

Focusing on the main features of nonhydrostatic, semi-implicit and semi-Lagrangian of GRAPES, the formulation of GRAPES global model and the polar discretization scheme are described in section 1, and the numerical results based on idealized tests are discussed in section 2. Conclusion and remarks are presented in section 3.

1 Polar discretization

1.1 Model equations

GRAPES model adopts a set of fully compressible nonhydrostatic equations on the sphere. It uses height-based terrain-following coordinate, has 2-level time semi-Lagrangian advection scheme and uses what is now a fairly standard semi-implicit time-integration scheme. Arakawa C grid with v at poles horizontally and Charney-Philips variable staggering vertically are employed. In order to accelerate the convergence of iteration, a preconditioned Generalized Conjugate Residual (GCR) algorithm is used to solve the three-dimensional Helmholtz equation for pressure perturbation, in which the reference atmospheric profile considers the terrain impacts. The model prognostic variables include perturbed Exner function π, perturbed potential temperature θ, horizontal velocity u, v and vertical velocity $\hat{w}$ as well as moisture varibales q. The nonhydrostatic equations on the spherical coordinates are given hereunder (for detailed schemes and variable definitions, see Chen D H, et al.[11]):

$$\pi = \xi_{\pi_1} u + \xi_{\pi_2} v + \xi_{\pi_3} \hat{w} + \xi_D (D_3)_{\hat{z}} + A_\pi, \tag{1}$$

$$u = \left[\xi_{u_1} \frac{1}{a\cos\varphi} \frac{\partial}{\partial \lambda} + \xi_{u_2} \frac{1}{a} \frac{\partial}{\partial \varphi} + \xi_{u_3} \frac{\partial}{\partial \hat{z}} \right] \pi + \xi_{u_0}, \tag{2}$$

$$v = \left[\xi_{v_1} \frac{1}{a\cos\varphi} \frac{\partial}{\partial \lambda} + \xi_{v_2} \frac{1}{a} \frac{\partial}{\partial \varphi} + \xi_{v_3} \frac{\partial}{\partial \hat{z}} \right] \pi + \xi_{v_0}, \tag{3}$$

$$\hat{w} = \left[\xi_{w_1} \frac{1}{a\cos\varphi} \frac{\partial}{\partial \lambda} + \xi_{w_2} \frac{1}{a} \frac{\partial}{\partial \varphi} + \xi_{w_3} \frac{\partial}{\partial \hat{z}} \right] \pi + \xi_{w_0}, \tag{4}$$

$$\theta = \xi_{\theta_3} \frac{\partial \pi}{\partial \hat{z}} + \xi_{\theta_0}, \tag{5}$$

$$q_i = \xi_{q_0}, \tag{6}$$

where q_i indicates the water substance considered in the model, which includes water vapor, cloud liquid water, cloud frozen water, other substance also can be added.

At the moment, the physical parameterization package of GRAPES is mainly introduced from WRF, which includes ECMWF's long and short-wave radiation schemes (Morcrette, 1989, 1998), cumulus convection (Betts Millers, 1986), cloud Microphysical scheme covering 3 simple ice categories from NCEP, NCEP's global MRF boundary-layer scheme (Hong and Pan, 1996), Blackadar's (1978B) land surface process, gravity wave drag (Miller, 1993, 1986), etc. Preliminary tests show that ECMWF's physical process is more suitable

to the medium-range model, for example the radiation scheme.

1.2 Determination of *v* at the two poles

As we know, most of operational global models adopt Arakawa B or C grid. But when the grid length is less than the radius of Rossby wave deformation, Arakawa C grids[12] is more applicable to the mesoscale flow. Xue et al.[13] also showed that Arakawa-C grid can better describe the geostrophic adjustment. Therefore, UKMO's new unified model and CMC's GEM model adopt this approach. But C grid has the following two variable staggering definitions in the poles: one is to put mass and *u* component (*u-h*) at the poles, as UKMO and CMC. The other is to put component *v* at the poles. The *u-h* is widely used in the modeling community by now. But for a model using semi-implicit and semi-Lagrangian advection scheme, the most difficulty of *u-h* staggering is the necessity to discrete all the prognostic variables at the poles except *v*, as well as three-dimensional divergence, vertical velocity, Helmholtz equation at the polar cap, etc. Comparatively, the second one only deals with *v* component at the poles. Evidently it is more easily implemented to *u-h* scheme. Thuburn et al.[14] pointed out that *v* rather than *u-h* at the poles had a better performance in kinetic energy conservation.

Therefore, the new developed GRAPES model puts *v* at poles. And there is only one prognostic variable *v* at the pole, without defining other variables, such as *u, w* and mass variables π, θ, etc. Thus it has greatly simplified the discretization computation.

v-component at poles is calculated diagnostically by applying the least squares minimization based on the *u*-component closest to the pole. For a uniform mesh ($\Delta\lambda$=const), as viewed form the earth's center, let the vector wind at the south pole have speed v_{SP} in the direction relative to the reference longitude $\lambda=\lambda_{1/2}=0$. In terms of this vector wind, the *v*-component of the wind at the south pole can be expressed as

$$v_{\lambda-1/2,-\pi/2} = V_{SP}\cos(\lambda_{i-1/2} - \lambda_{SP}), \tag{7}$$

where $i = 1, 2, ..., L,\ A = -\frac{2}{L}\sum_{i=1}^{L} u_{i,1}\sin\lambda_i,$

$$B = \frac{2}{L}\sum_{i=1}^{L}\Delta u_{i,1}\cos\lambda_i.$$

For uniform mesh, $\Delta\lambda = 2\pi/L$, in which L is the number of grids in the X direction.

Similarly, the *v*-component at the north pole:

$$v_{\lambda-1/2,\pi/2} = V_{NP}\cos(\lambda_{i-1/2} - \lambda_{NP}), \tag{8}$$

where $\lambda_{NP} = \tan^{-1}\left(\frac{B}{A}\right),\ v_{NP} = \sqrt{A^2 + B^2}$,

$$A = \frac{2}{L}\sum_{i=1}^{L} u_{i,1}\sin\lambda_i,\ \ B = -\frac{2}{L}\sum_{i=1}^{L} u_{i,1}\cos\lambda_i.$$

For GRAPES global model, the lateral boundary conditions in the east-west or λ direction are those of periodicity. For scalar variables, in the case of points lying in the immediate neighborhood of the poles, then it uses values at grid points lying on the other side of the poles. Whenever vector component from across the poles are used, they should undergo a change of sign. Moreover, for semi-Lagrangian departure point calculation, additional 5 grids are extended from the predicted domain along *x* and *y* directions, thus a halo area is formed.

1.3 Polar filtering

For a grid point model formulated on spherical coordinate, the horizontal grid length in the east-west direction becomes very small as the pole is approached. Consequently, near to the poles, the model may suffer from the presence of small scale, these signals can be transported away from the pole where they rapidly become grid scale and contaminate the resolved response in these regions. In addition, noise at the grid scale can significantly slow down the convergence of the Helmholtz solver. Moreover, when the model takes a longer time step, computational instability may occur at higher latitudes. Except decreasing time step, another commonly used method is to filter these unstable wave components at higher latitude. Wang et al.[10] used an equal-area grid to alleviate this phenomenon in GAMIL global grid-point model.

Currently, GRAPES uses the following scheme. For an arbitrary variable Q, the filter operator is formally written as

$$\frac{\partial Q}{\partial t} = \frac{K_p}{a^2\cos^2\varphi}\frac{\partial^2 Q}{\partial\lambda^2}, \tag{9}$$

where K_p is the filter coefficient. The explicit discrete expression can be expressed as

$$\begin{aligned} Q^f_{i,j,k} &= P(Q^n_{i,j,k}) = Q^n_{i,j,k} \\ &\quad + K(Q^n_{i+1,j,k} - 2Q^n_{i,j,k} + Q^n_{i-1,j,k}), \end{aligned} \tag{10}$$

where Q^f indicates the filtered field.

In the model, K is set to equal 1/4. Polar filtering is

applied at the beginning of each time step in the region of the north pole or south pole for latitudes greater than 80° or less than –80°.

1.4 Treatment of Helmholtz equation at the poles

Concerning a semi-implicit time integration model, it is necessary to solve a three-dimensional Helmholtz equation containing cross terms. Discretized v and π equations are written as

$$v = \xi_{v_1}\left(\overline{\pi}^{\lambda\varphi}\right)_\lambda + \xi_{v_2}\pi_\varphi + \xi_{v_3}\left(\overline{\pi}^{\hat{z}\varphi}\right)_{\hat{z}} + \xi_{v_0}, \tag{11}$$

$$\begin{aligned}\pi = {} & \xi_{\pi_1}\overline{u}^{\lambda} + \xi_{\pi_2}\overline{v}^{\varphi} + \xi_{\pi_3}\overline{\hat{w}}^{\hat{z}} \\ & + \xi_{\pi_D}\left[u_\lambda + \frac{1}{\cos\varphi}(v\cos\varphi)_\varphi + \hat{w}_{\hat{z}}\right] + A_\pi.\end{aligned} \tag{12}$$

So

$$\begin{aligned}\pi = {} & \overline{\xi_{\pi_1}(\xi_{u_1}\pi_\lambda + \xi_{u_2}(\overline{\pi}^{\varphi\lambda})_\varphi + \xi_{u_3}(\overline{\pi}^{\hat{z}\lambda})_{\hat{z}} + \xi_{u_0})}^{\lambda} \\ & + \overline{\xi_{\pi_2}(\xi_{v_1}(\overline{\pi}^{\lambda\varphi})_\lambda + \xi_{v_2}\pi_\varphi + \xi_{v_3}(\overline{\pi}^{\hat{z}\varphi})_{\hat{z}} + \xi_{v_0})}^{\varphi} \\ & + \overline{\xi_{\pi_3}(\xi_{w_1}(\overline{\pi}^{\hat{z}\lambda})_\lambda + \xi_{w_2}(\overline{\pi}^{\hat{z}\varphi})_\varphi + \xi_{w_3}\pi_{\hat{z}} + \xi_{w_0})}^{\hat{z}} \\ & + \xi_{\pi_D}\left[\left(\xi_{u_1}\pi_\lambda + \xi_{u_2}(\overline{\pi}^{\varphi\lambda})_\varphi + \xi_{u_3}(\overline{\pi}^{\hat{z}\lambda})_{\hat{z}} + \xi_{u_0}\right)_\lambda + \frac{1}{\cos\varphi}\cdot\right. \\ & \left\{\cos\varphi\left(\xi_{v_1}(\overline{\pi}^{\lambda\varphi})_\lambda + \xi_{v_2}\pi_\varphi + \xi_{v_3}(\overline{\pi}^{\hat{z}\varphi})_{\hat{z}} + \xi_{v_0}\right)\right\}_\varphi \\ & \left. + \left(\xi_{w_1}(\overline{\pi}^{\hat{z}\lambda})_\lambda + \xi_{w_2}(\overline{\pi}^{\hat{z}\varphi})_\varphi + \xi_{w_3}\pi_{\hat{z}} + \xi_{w_0}\right)_{\hat{z}}\right] + A_\pi.\end{aligned} \tag{13}$$

Helmholtz equation (13) is solved by substituting the discretized u, v, w equations into π equation (12). At the pole point, as both meridional and zonal derivatives do not exist, variable v needs to be computed diagnostically. Thus, when the grid reaches to the nearest latitude to the pole, $v_{i,p}^{n+1}$ at the pole in eq. (12) is time extrapolated approximately:

$$v_{i,p}^{n+1} = 2v_{i,p}^{n} - v_{i,p}^{n-1},$$

where p represents polar region, and n is the current time step. Thus, Helmholtz equation for the nearest circle to the pole is transformed into the following expression:

$$\begin{aligned}\pi = {} & \overline{\xi_{\pi_1}(\xi_{u_1}\pi_\lambda + \xi_{u_2}(\overline{\pi}^{\varphi\lambda})_\varphi + \xi_{u_3}(\overline{\pi}^{\hat{z}\lambda})_{\hat{z}} + \xi_{u_0})}^{\lambda} \\ & + \frac{1}{2}\xi_{\pi_2}\left(\xi_{v_1}(\overline{\pi}^{\lambda\varphi})_\lambda + \xi_{v_2}\pi_\varphi + \xi_{v_3}(\overline{\pi}^{\hat{z}\varphi})_{\hat{z}} + \xi_{v_0}\right) \\ & + \overline{\xi_{\pi_3}(\xi_{w_1}(\overline{\pi}^{\hat{z}\lambda})_\lambda + \xi_{w_2}(\overline{\pi}^{\hat{z}\varphi})_\varphi + \xi_{w_3}\pi_{\hat{z}} + \xi_{w_0})}^{\hat{z}} \\ & + \xi_{\pi_D}\left[\left(\xi_{u_1}\pi_\lambda + \xi_{u_2}(\overline{\pi}^{\varphi\lambda})_\varphi + \xi_{u_3}(\overline{\pi}^{\hat{z}\lambda})_{\hat{z}} + \xi_{u_0}\right)_\lambda + \frac{1}{\cos\varphi}\cdot\right. \\ & \left\{\cos\varphi\left(\xi_{v_1}(\overline{\pi}^{\lambda\varphi})_\lambda + \xi_{v_2}\pi_\varphi + \xi_{v_3}(\overline{\pi}^{\hat{z}\varphi})_{\hat{z}} + \xi_{v_0}\right)\right\}_\varphi \\ & \left. + \left(\xi_{w_1}(\overline{\pi}^{\hat{z}\lambda})_\lambda + \xi_{w_2}(\overline{\pi}^{\hat{z}\varphi})_\varphi + \xi_{w_3}\pi_{\hat{z}} + \xi_{w_0}\right)_{\hat{z}}\right] + A_\pi^p,\end{aligned} \tag{14}$$

in which $A_\pi^p = \frac{1}{2}\xi_{\pi_2}v_{i,p} + A_\pi$.

1.5 Semi-Lagrangian computations near the poles

As mentioned above, the prognostic variables in GRAPES model include Exner function, potential temperature, horizontal component u and v, vertical velocity and moisture variables. The model adopts Arakawa C horizontally and Charney-Phillips vertically and uses 2-level time semi-Lagrangian scheme.

As GRAPES formulated on spherical coordinate, the unit vector of u and v component at the departure point and arrival point along the Lagrangian trajectory is different. Therefore, the vector discretization method[15] is employed to calculate Lagrangian departure point in the model. As horizontal u, v and w are located at respective grid points, the vertical wind w and potential temperature θ are at the same layer, while u, v and θ are located between the two w levels. Thus, such a distribution has 4 sets of departure points: u, v, w (θ) and π.

In the model, the procedure of Ritche and Beaudoin's[16] is used to find the departure point corresponding to all latitudes equatorwards of 80°N and 80°S. As the expression to compute departure points contains a second-order term in GRAPES, this makes the calculations more precise, in which the accuracy of λ reaches Δt^5 and that of φ reaches Δt^4. When the model grid point is located at poleward of 80°, as terms in $\tan\varphi_a$ and $\sec\varphi_a$ may appear in Ritchie and Beaudoin's scheme, so the model takes rotated-grid approach of McDonald and Bates[17] to locate departure point.

The following interpolation options are offered in GRAPES model, such as linear, cubic-Lagrangian, quasi-cubic Lagrangian interpolation schemes. Cubic interpolation is applied in the interior, while linear interpolation is applied in all gird boxes adjacent to the boundary. To prevent occurrence of negative moisture[18], a linear positive definite interpolation method is applied in moisture variables. Both during and after iteration to find departure and midpoints, checks are made to ensure that they do not lie outside the domain. If midpoints and

departure points found to be out of bounds, they will be relocated to the appropriate model level. In order to maintain the conservation and monotonicity[19], the scheme of Bermejo and Staniforth[20] approach is used to curb any fictitious overshoots.

2 Results

2.1 Balance flow tests

For a Lagrangian model, the Lagrangian trajectory calculation is the basis of the whole dynamic core of the model. It is closely related to the rationality and accuracy of the advection calculations. The idealized balance flow test is an effective method to validate the dynamic framework. Any mistreatment of this may lead to distort its balance structure.

Assuming $v=0$, $\hat{w}=w\equiv 0$, u component satisfies the geostrophic balance:

$$\frac{C_P\theta}{a}\frac{\partial\pi}{\partial\varphi}=-2\Omega\sin\varphi\cdot u-\frac{u^2}{a}\tan\varphi, \tag{15}$$

where potential temperature and pressure variable π meets the hydrostatic assumption:

$$C_P\theta\frac{\partial\pi}{\partial z}=-g. \tag{16}$$

Meanwhile, the potential temperature also satisfies

$$\frac{1}{\theta}\frac{\partial\theta}{\partial z}=\frac{N^2}{g}, \tag{17}$$

where N is the Brunt-Väisällä frequency, and $u = u_0\cos\varphi$. According to the characteristics of Lagrangian air parcel moving along the trajectory, without topography, the parcel structures of zonal wind will not change during the integration. Figure 1 gives GRAPES's initial field of zonal wind and the results after 1000 days integration. The horizontal resolution is 0.5° and the time step is 1 hour. From Figure 1, it can be noted clearly that the trajectory of component u still retains straight as the initial does. This indicates the rationality and stability of the treatment of semi-Lagrangian calculation and the disposal of polar discretization scheme.

2.2 Model conservation verification

As a global medium-range numerical prediction model, the conservation property is one of the most important criterions to validate the performance of the model. Held and Suarez[21] (HS for short) designed an idealized forced test to try to compare different dynamical formulations without the complication of physics parameterizations for assessing the statistic characteristics of long-time three-dimensional global circulation model integration, which has been extensively used for global

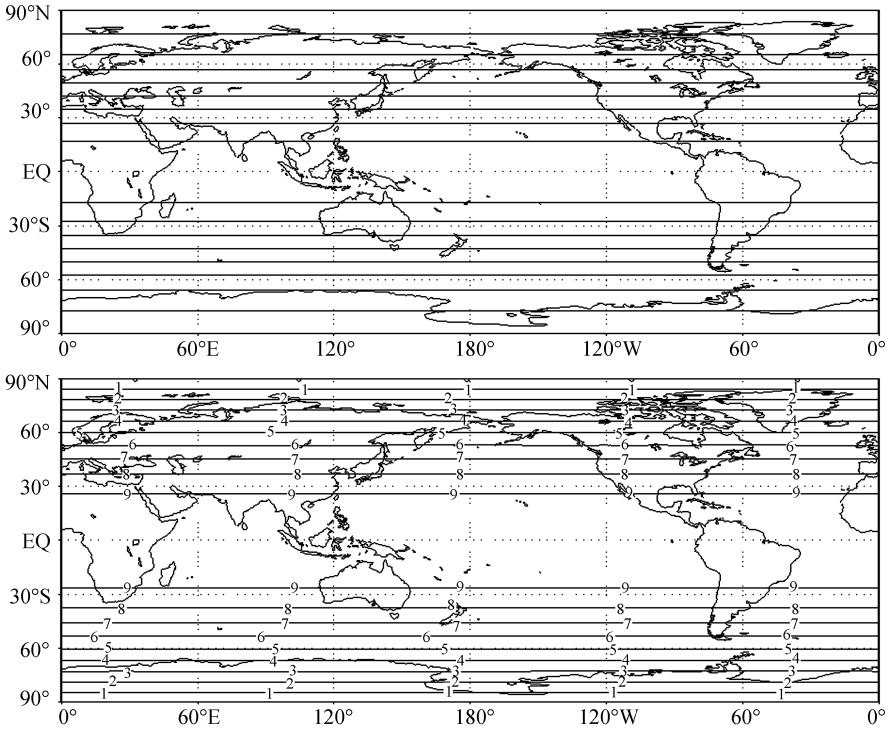

Figure 1 The evolution of u component: initial field (top) after 1000 days integration (bottom).

model verifications. Therefore, HS was used as a benchmark to verify its conservation performance for long time integration of GRAPES model.

Test scheme:

$$\frac{\partial v}{\partial t} = -k_v(\sigma)_v, \tag{18}$$

$$\frac{\partial T}{\partial t} = -k_T(\varphi,\sigma)\left[T - T_{eq}(\varphi,p)\right], \tag{19}$$

in which

$$T_{eq} = \max\left\{200K, \left[315 - (\Delta T)_y \sin^2\varphi - (\Delta\theta)_z \log\left(\frac{p}{p_0}\right)\cos^2\varphi\right]\left(\frac{p}{p_0}\right)^{\kappa}\right\},$$

$$k_T = k_a + (k_s - k_a)\max\left(0, \frac{\sigma-\sigma_b}{1-\sigma_b}\right)\cos^4\phi,$$

$$k_v = k_f \max\left(0, \frac{\sigma-\sigma_b}{1-\sigma_b}\right),$$

other parameters are set to

$$k_f = 1\text{day}^{-1},\ k_a = 1/40\text{day}^{-1},\ k_s = 1/4\ \text{day}^{-1}$$

$$\sigma_b = 0.7,\ (\Delta T)_y = 60K,\ (\Delta\theta)_z = 10K.$$

The model is then run on a smooth planet with a simple surface friction and a prescribed temperature relaxation to produce an equator-pole temperature gradient and a realistic vertical structure. In the test, the horizontal resolution is 2.5° with 17 vertical levels and the time step is 1800 seconds. Figure 2(a)—(c) give the evolution of relative error for total energy, total kinetic energy and total mass after integration for 1000 days. And the model is adiabatic, no physical parameterization schemes are involved. It can be seen that the conservation properties of GRAPES global model are quite good in terms of total energy, total kinetic energy and total mass.

3 Discussion and conclusions

GRAPES, a nonhydrostatic semi-implicit and semi-Lagrangian global model, which was developed during the past 5 years, will be run operationally by CMA in 2010. The dynamic core of the model adopts a set of nonhydrostatic and fully compressible equations formulated on spherical coordinate with latitude and longitude, and uses height-based terrain following coordinate. The model employs hydrostatic assumption reference profile, semi-implicit and semi-Lagrangian in 2-level time integration. The spatial differential adopts Arakawa

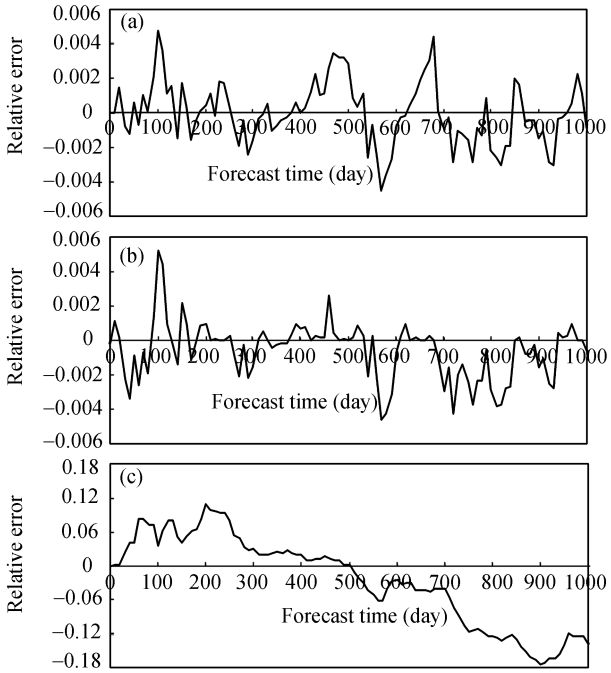

Figure 2 The time evolution of relative error for (a) total energy (b) total kinetic energy (c) global mass.

C grid with v at poles, and Charney-Philips variable staggering in the vertical. The pre-conditioned generalized conjugate residual (GCR) method is used to solve the three-dimensional Helmholtz equation for pressure perturbation.

Focusing on the characteristics of semi-implicit and semi-Lagrangian model, this paper describes the model scheme as well as the polar discretization scheme. To validate the consistency and stability of GRAPES numerical schemes, an idealized balance flow test is designed to verify the correctness of the polar discretization and code programming. HS tests show that GRAPES has a very good conservation property during long-time integration.

And these have established a solid foundation for operational implementation. In the next 2 or 3 years, we will conduct a large amount of sensitive tests to determine the appropriate physical parameterization schemes suitable for global GAREPS model to improve the predictability of the model. Meanwhile, the conversation consideration for climate modeling is also will be focused.

The authors sincerely thank Ji Liren (*Institute of Atmospheric Physic, CAS*), *Xue Jishan* (*Chinese Academy of Meteorological Sciences*) *and others for their constructive comments and suggestions during the model designing and development.*

1 Ritchie H, Temperton C, Simmons A, et al. Implementation of the semi-Lagrangian method in a high resolution of the ECMWF forecat model. Mon Wea Rev, 1995, 123: 489－514
2 Kalnay, Kanamitsu M, Baker W E. Global numerical weather prediction at the National Meteorological Center. Bull Amer Meteor Soc, 1990, 71: 1410－1428
3 Bubnova, Gello R G, Bernard P, et al. Integration of the fully elastic equations cast in hydrostatic pressure terrain-following coordinate in the framework of the ARPEGE/ALADIN NWP system. Mon Wea Rev, 1995, 123: 515－535
4 Wu G X, Liu H, Zhao Y C, et al. A nine-layer atmospheric general circulation model and its performance. Adv Atmos Sci, 1996, 13: 1－18
5 Yang X S, Song J Q. The multi-tasking concurrent computing of medium-range numerical weather prediction model T63L16 on Galaxy-2 supercomputer. Quar J App Meteor (in Chinese), 1997, 7(4): 331－336
6 Chen Q Y, Yao M M, Wang Y. A new generation of operational medium-range weather forecast model T213L31 in National Meteorological Center. Meteor Mon (in Chinese), 2004, 30(10): 16－21
7 Ji L R, Chen J B, Zhang D M, et al. Review of some numerical aspects of the dynamic framework of NWP Model. Chin J Atmos Sci (in Chinese), 2005, 29(1): 120－130
8 Staniforth A, White A, Wood N, et al. Developing efficient unified nonhydrostatic models. UKMO, Personal communication
9 Cote J, Gravel S, Methot A, et al. The operational CMC-MRB Global Environmental Multiscale (GEM) model. Part I: Design considerations and formulation. Mon Wea Rev, 1998, 126: 1373－1395
10 Wang B, Wan H, Ji Z Z, et al. Design of a new dynamical core for global atmospheric models based on some efficient numerical methods. Sci China Ser A-Mathematics, 2004, 47 (Supp.): 4－21
11 Chen D H, Xue J S, Yang X S, et al. The new generation of hydrostatic/nonhydrostatic multi-scales numerical prediction model: Scientific design and experiments. CAMS Technical Report 1 (in Chinese). 2003, 1－230
12 Cullen M J P, Davies T, Mawson M H, et al. An overriew of numerical methods for the next generation of NWP and climate models. In: Lin C, Laprise R, Ritchie H, eds. The Andre Robert Memorial Volume. Can Meteor Ocean Soc, 1997, 425－444
13 Xue M, Droegemeier K K, Wong V. The advanced regional prediction System (ARPS)——A multi-scale nonhydrostatic atmospheric simulation and prediction model. Part I: Model dynamics and verification. Meteor Atmos Phys, 2000, 75: 161－193
14 Thuburn J, Staniforth A. Conservation and linear Rossby-Mode dispersion on the spherical C grid. Mon Wea Rev, 2004, 132: 641－653
15 Bate J R, Semazzi F H M, Higgins, et al. Integration of the shallow water equation on the sphere using a semi-Lagrangian scheme with a multigrid solver. Mon Wea Rev, 1990, 118: 1615－1627
16 Ritche H, Beaudoin C. Approximation and sensitivity experiments with a baroclinic semi-Lagrangian spectral model. Mon Wea Rev, 1994, 116: 1587－1598
17 McDonald A, Bates J R. Semi-Lagrangian integration of a gridpoint shallow water model on the sphere. Mon Wea Rev, 1989, 117: 130－137
18 Chen J B, Ji Z Z. A Study of complete square-conserving semi-implicit semi-lagrangian scheme. Chin J Atmos Sci (in Chinese), 2004, 28(4): 527－535
19 Bermejo R, Staniforth A. The conversion of semi-Lagrangian advection schemes to quasi-monotone schemes. Mon Wea Rev, 1992, 120: 2622－2632
20 Wang B, Ji Z Z. Construction and numerical tests of the multi conversation difference scheme. Chin Sci Bull, 2003, 48(10): 1016－1020
21 Held I M, Suarez M J. A proposal for the intercomparison of the dynamical cores of atmospheric general circulation models. Bull Amer Meteor Soc, 1994, 75(10): 1825－1830